Measurement of jet production with the ATLAS detector

Gino Marceca

Universidad de Buenos Aires

PHENOEXP-2018, 9 May 2018

Outline

Inclusive-jet and dijet cross-sections at 13 TeV

arXiv:1711.02692
(7th November 2017)

Overview (Jet cross-sections at 13 TeV)

- Measurement of the inclusive-jet and dijet cross sections at 13 TeV with an integrated luminosity of 3.2 fb^{-1}.
- Measured cross-sections are compared to NLO QCD calculations corrected for non-perturbative and electroweak effects.
- Level of agreement with NLO predictions is quantified via a χ^2 test.
- Qualitative comparison with the recent NNLO QCD calculations for inclusive-jet cross-section at 13 TeV.

Event Reconstruction and Selection

- Jets reconstructed using the anti-k_t algorithm, with a radius parameter value of R=0.4.
- Jets calibrated using Monte Carlo simulation and data-driven methods.

Analysis	**Selection**	**Phase-space**
Inclusive-jet @13 TeV	$\|y\| < 3.0$ $p_{\mathrm{T}} > 100$ GeV	$\|y\| < 3.0$ p_{T} : $100 - 3500$ GeV
Dijet @13 TeV	$y^* < 3.0$ $\mathrm{p_{T_2}} > 75$ GeV $\mathrm{H_{T2}} = (p_{T_1} + p_{T_2}) > 200$ GeV	$y^* < 3.0$ m_{jj} : $300 - 9000$ GeV

$y^* = \left|y_1 - y_2\right|/2$ where 1,2 subscripts label the highest and second highest p_{T} jet within $|y| < 3.0$

Cross-section definition

The **inclusive-jet** cross-section is measured as a function of the jet p_{T}, in six absolute jet rapidity $|y|$ bins:

$$|y| < 0.5, \quad 0.5 \leq |y| < 1.0, \quad 1.0 \leq |y| < 1.5,$$
$$1.5 \leq |y| < 2.0, \quad 2.0 \leq |y| < 2.5, \quad 2.5 \leq |y| < 3.0.$$

The **dijet** cross-section is measured as a function of the dijet invariant mass, in six y^* bins:

$$y^* < 0.5, \quad 0.5 \leq y^* < 1.0, \quad 1.0 \leq y^* < 1.5,$$
$$1.5 \leq y^* < 2.0, \quad 2.0 \leq y^* < 2.5, \quad 2.5 \leq y^* < 3.0.$$

Trigger

Trigger Data is selected using several jet transverse energy thresholds.

Trigger strategy Inclusive combination of single-jet triggers. arXiv:0901.4118

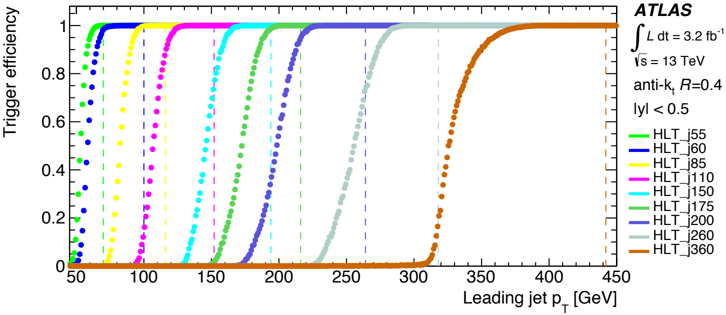

reference here

- The trigger efficiency is equal to or above 99.9% in the p_T range where it was considered.

Monte Carlo Generators

Pythia, Sherpa, Powheg and Herwig++ MC generators[1] used for:

- Deconvolution of detector effects (unfolding) (Pythia and Sherpa).
- Evaluation of non-perturbative (NP) corrections (Pythia).
- Estimation of NP correction uncertainties (Pythia and Herwig++).
- Propagation of experimental systematic uncertainties (Pythia and Powheg).

[1] The MC versions and PDF sets used for each generator are detailed in the backup

NP corrections at 13 TeV

Considers effects from underlying-event and hadronisation.

- $C_{NP} = \frac{MC(UE\ ON, HAD\ ON)}{MC(UE\ OFF, HAD\ OFF)}$

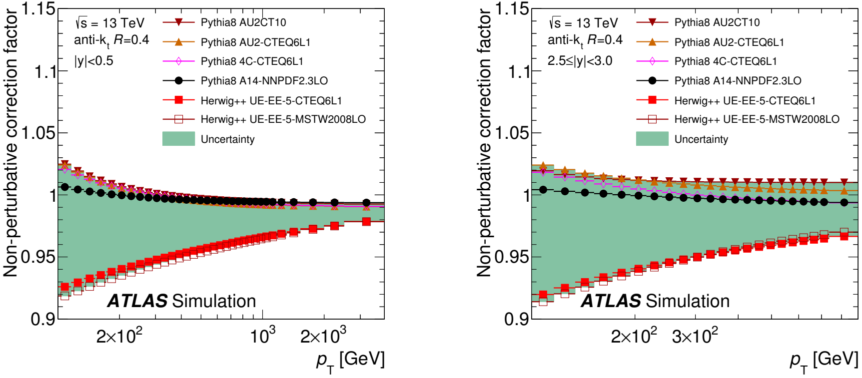

Bayesian Unfolding

- Iterative Dynamically Stabilised (IDS) method used to correct reconstructed spectra for detector inefficiencies and resolution effects.
- Based on a transfer matrix (TM) constructed using simulated events.
- Inclusive-jet: the TM is filled jet by jet by matching a reco jet with a particle-level jet within a radius of $R = 0.3$.
- Dijet: the TM is filled event by event when lying in the same y^* bin.

p_T Transfer Matrix

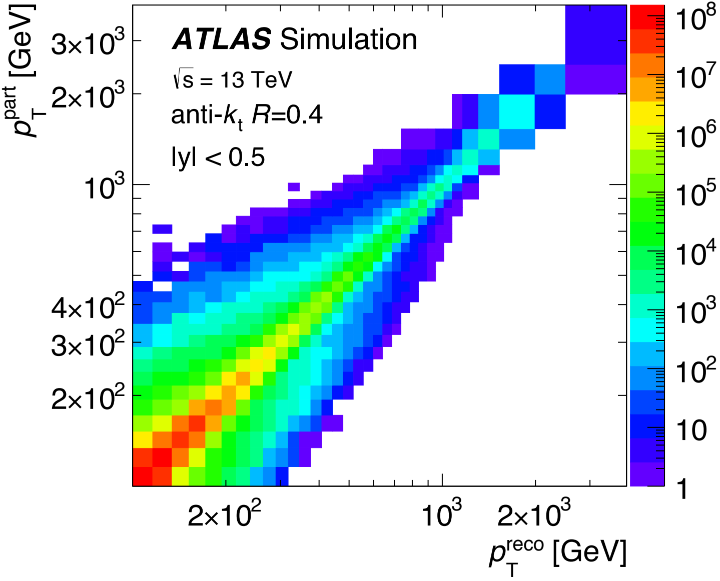

reference here

Theoretical Predictions

- QCD calculations: Done with NLOJet++ plus non-perturbative and electroweak corrections

Nominal scale choices:

- Inclusive-jet: leading jet p_T (p_T^{max}).
- Dijet: $p_T^{max} e^{0.3y^*}$

PDFs: CT14, NNPDF 3.0, MMHT14, HERAPDF 2.0, ABMP16.

Uncertainties in the NLO calculation:

- (μ_R, μ_F) scale variations (dominant at low p_T).
- PDFs (dominant at high p_T).
- α_s variation (mostly constant in all p_T and $|y|$ ranges considered).

Additional theoretical uncertainty:

- Alternative scale choice based on each jet p_T (p_T^{jet}). Difference w.r.t to p_T^{max} was treated as an uncertainty.

NLO QCD uncertainties at 13 TeV

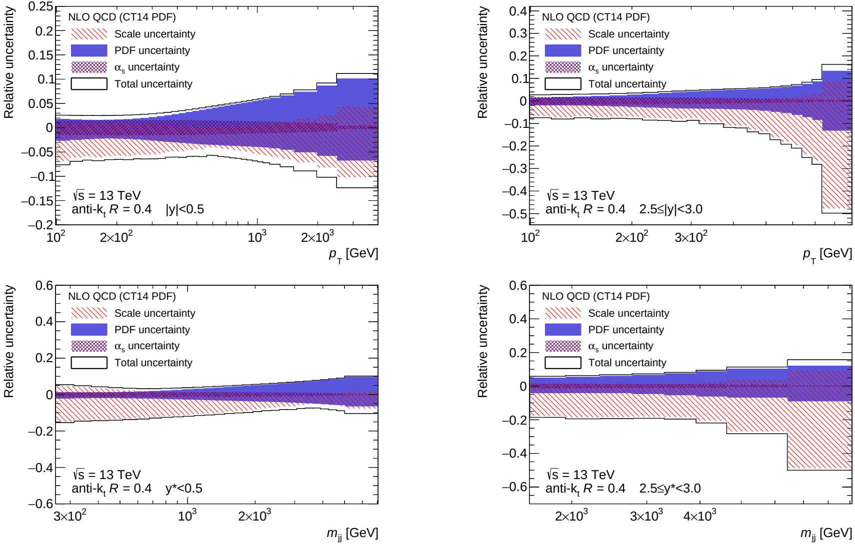

Results: Cross-section comparison

7 TeV (arXiv:1410.8857)

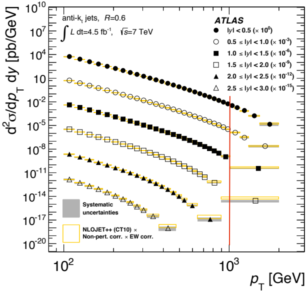

8 TeV (arXiv:1706.03192)

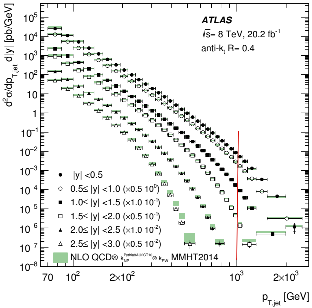

13 TeV

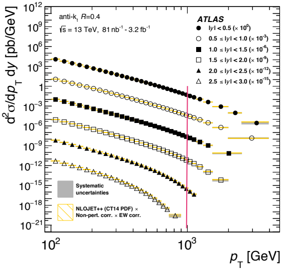

- 7 TeV result shown as a comparison with 8 and 13 TeV.
- Significant improvement in systematics and range w.r.t 7 TeV measurement.
- Greater p_T range reached by 13 TeV w.r.t 8 TeV.

Results: NLOJet++ vs Unfolded Data (Incl-jet 13 TeV)

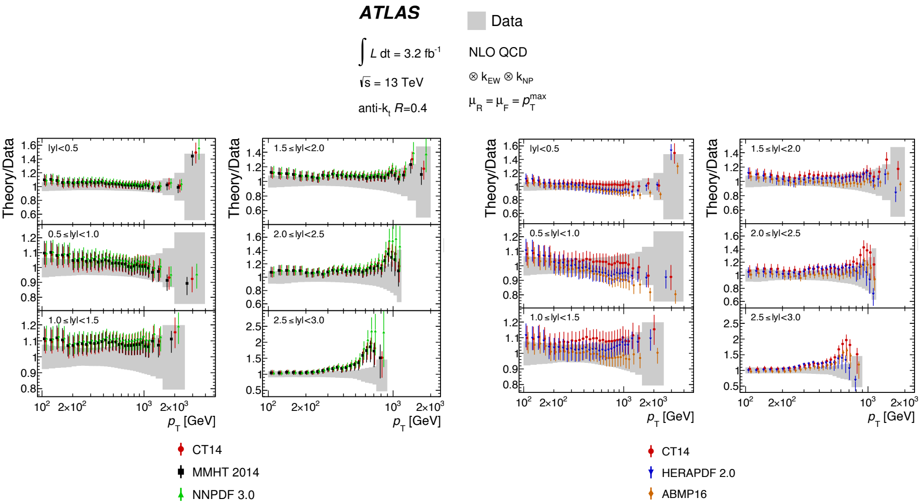

- NNPDF, CT14 and MMHT overestimate the cross-section for the last two $|y|$ bins.

Results: NLOJet++ vs Unfolded Data (Dijet 13 TeV)

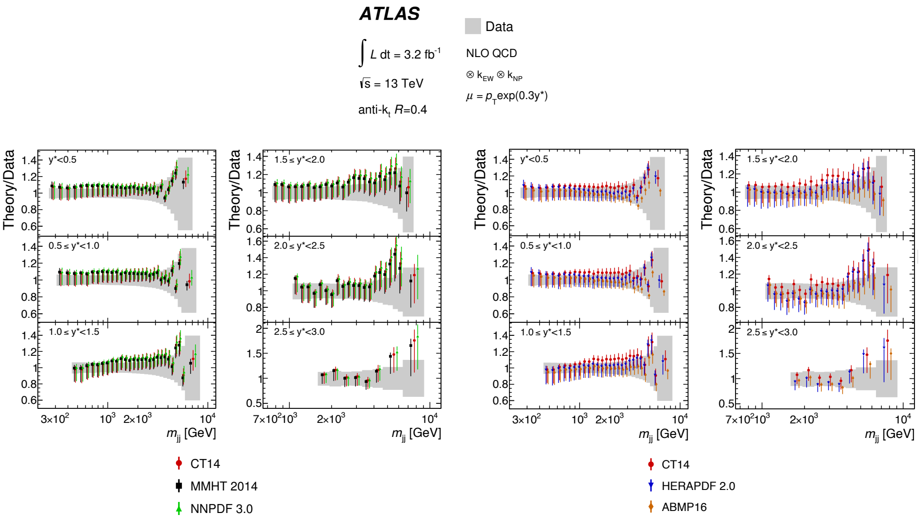

Results: NNLOJet vs Unfolded Data

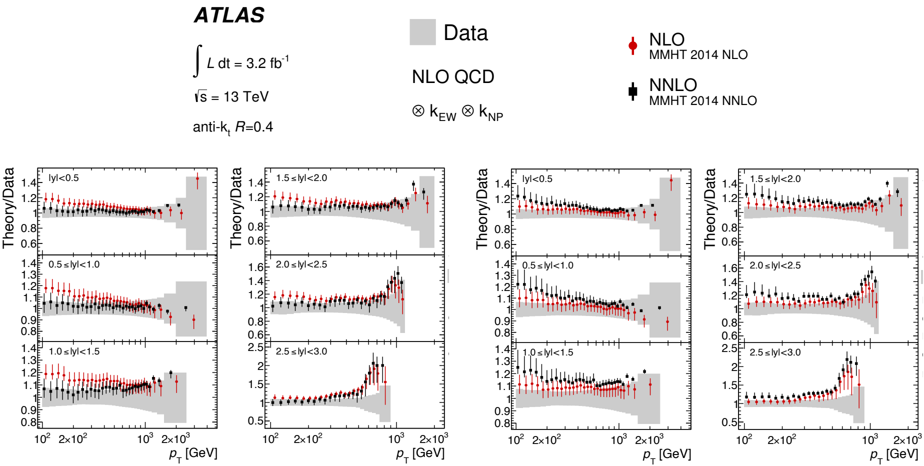

$\mu_R = \mu_F = p_T^{jet}$

$\mu_R = \mu_F = p_T^{max}$

This is what we want

This is not what we want

Results: p-values w.r.t NLO (Inclusive-jet 13 TeV)

	P_{obs}				
Rapidity ranges	CT14	MMHT 2014	NNPDF 3.0	HERAPDF 2.0	ABMP16
$p_{\mathrm{T}}^{\mathrm{max}}$					
$\lvert y\rvert < 0.5$	67%	65%	62%	31%	50%
$0.5 \leq \lvert y\rvert < 1.0$	5.8%	6.3%	6.0%	3.0%	2.0%
$1.0 \leq \lvert y\rvert < 1.5$	65%	61%	67%	50%	55%
$1.5 \leq \lvert y\rvert < 2.0$	0.7%	0.8%	0.8%	0.1%	0.4%
$2.0 \leq \lvert y\rvert < 2.5$	2.3%	2.3%	2.8%	0.7%	1.5%
$2.5 \leq \lvert y\rvert < 3.0$	62%	71%	69%	25%	55%

Results: global fits (Inclusive-jet 13 TeV)

χ^2/dof all $\|y\|$ bins	CT14	MMHT 2014	NNPDF 3.0	HERAPDF 2.0	ABMP16
$p_{\mathrm{T}}^{\mathrm{max}}$	419/177	431/177	404/177	432/177	475/177
$p_{\mathrm{T}}^{\mathrm{jet}}$	399/177	405/177	384/177	428/177	455/177

- Strong tensions (p-values $\ll 10^{-3}$) observed when considering all jet p_{T} and $|y|$ regions. Similar pattern present also at 8 TeV.
- Numerous studies on the correlation of the systematic sources were done but the tension remains.

Results: p-values (Dijets 13 TeV)

	P_{obs}				
y^* ranges	CT14	MMHT 2014	NNPDF 3.0	HERAPDF 2.0	ABMP16
$y^* < 0.5$	79%	59%	50%	71%	71%
$0.5 \leq y^* < 1.0$	27%	23%	19%	32%	31%
$1.0 \leq y^* < 1.5$	66%	55%	48%	66%	69%
$1.5 \leq y^* < 2.0$	26%	26%	28%	9.9%	25%
$2.0 \leq y^* < 2.5$	43%	35%	31%	4.2%	21%
$2.5 \leq y^* < 3.0$	45%	46%	40%	25%	38%
all y^* bins	8.1%	5.5%	9.8%	0.1%	4.4%

- As opposed to the inclusive case, good agreement when considering all y^* bins together.

Conclusions: Inclusive-jet and dijet analyses

- The measurements of the inclusive jet and dijet cross-sections at 13 TeV was presented.
- The Data were collected with the ATLAS detector during 2015 corresponding to an integrated luminosity of $3.2\,\text{fb}^{-1}$.
- Quantitative(Qualitative) comparisons between data and NLO(NNLO) pQCD calculations, corrected by NP and EW effects, were performed.
- Fair agreement when considering jet cross-sections in individual $|y|$,y^* bins independently.
- Tensions between data and theory observed when considering data from all jet p_{T} and $|y|$ regions.
- No significant deviations between data and NNLO when using $p_{\mathrm{T}}^{\mathrm{jet}}$ scale.
- NNLO overestimates the cross-sections when using $p_{\mathrm{T}}^{\mathrm{max}}$ scale.

back-up slides

Monte Carlo Generators @8TeV & @13TeV

- Simulated events using the Pythia v8.160(v8.186) MC generator with CT10(NNPDF 2.3) LO PDF and AU2(A14) tune.
- Evaluation of non-perturbative uncertainties: Pythia v8.186 and Herwig++ v2.7.1.

Experimental uncertainties @13 TeV

- The Jet Energy Scale, Jet Energy Resolution and Luminosity uncertainties were estimated and taken into account using MC and data-driven techniques.
- The JES is the dominating uncertainty.

inclusive-jet

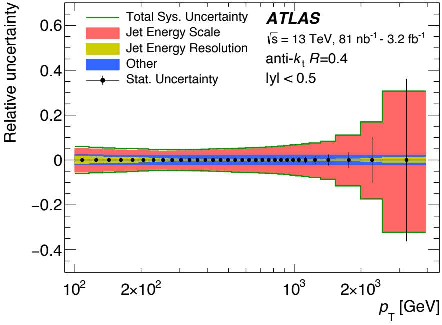

dijet

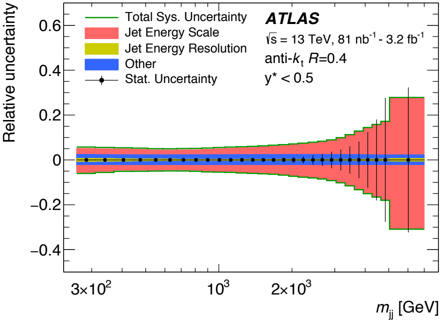

Systematics: Correlation Studies at 13 TeV

- To test in a realistic way the sensitivity to the correlations, alternative scenarios were provided for the two-point systematics.
- A complete description of these studies can be found in the 8 TeV measurement arXiv:1706.03192.
- Different options for splitting the systematics in sub-components as a function of p_{T} and $|y|$ where studied.
- For the theoretical uncertainties 3 other splitting options were tried as discussed here.
- The χ^2 is reduced by up to 58 units by splitting both the theoretical and experimental uncertainties.
- Despite this, the corresponding p_{obs} values are still $\ll 10^{-3}$

Systematics: Correlation Studies at 13 TeV

Summary of the 18 options for splitting the two-point systematic uncertainties into two (first 12) or three (last 6) sub-components:

Splitting option	Sub-component(s) definition(s), completed by complementary
1	$L(\ln(p_T[\text{TeV}]), \ln(0.1), \ln(2.5))\cdot$ uncertainty
2	$L(\ln(p_T[\text{TeV}]), \ln(0.1), \ln(2.5)) \cdot 0.5\cdot$ uncertainty
3	$L(p_T[\text{TeV}], 0.1, 2.5)\cdot$ uncertainty
4	$L(p_T[\text{TeV}], 0.1, 2.5) \cdot 0.5\cdot$ uncertainty
5	$L((\ln(p_T[\text{TeV}]))^2, (\ln(0.1))^2, (\ln(2.5))^2)\cdot$ uncertainty
6	$L((\ln(p_T[\text{TeV}]))^2, (\ln(0.1))^2, (\ln(2.5))^2) \cdot 0.5\cdot$ uncertainty
7	$L(\|y\|, 0, 3)\cdot$ uncertainty
8	$L(\|y\|, 0, 3) \cdot 0.5\cdot$ uncertainty
9	$L(\ln(p_T[\text{TeV}]), \ln(0.1), \ln(2.5)) \cdot L(\|y\|, 0, 3)\cdot$ uncertainty
10	$L(\ln(p_T[\text{TeV}]), \ln(0.1), \ln(2.5)) \cdot \sqrt{1 - L(\|y\|, 0, 3)^2}\cdot$ uncertainty
11	$L(\ln(p_T[\text{TeV}]), \ln(0.1), \ln(2.5)) \cdot L(\|y\|, 0, 3) \cdot 0.5\cdot$ uncertainty
12	$L(\ln(p_T[\text{TeV}]), \ln(0.1), \ln(2.5)) \cdot \sqrt{1 - L(\|y\|, 0, 3)^2} \cdot 0.5\cdot$ uncertainty
13	$L(\ln(p_T[\text{TeV}]), \ln(0.1), \ln(2.5)) \cdot \sqrt{1 - L(\|y\|, 0, 1.5)^2}\cdot$ uncertainty $L(\ln(p_T[\text{TeV}]), \ln(0.1), \ln(2.5)) \cdot L(\|y\|, 1.5, 3)\cdot$ uncertainty
14	$L(\ln(p_T[\text{TeV}]), \ln(0.1), \ln(2.5)) \cdot \sqrt{1 - L(\|y\|, 0, 1)^2}\cdot$ uncertainty $L(\ln(p_T[\text{TeV}]), \ln(0.1), \ln(2.5)) \cdot L(\|y\|, 1, 3)\cdot$ uncertainty
15	$L(\ln(p_T[\text{TeV}]), \ln(0.1), \ln(2.5)) \cdot \sqrt{1 - L(\|y\|, 0, 2)^2}\cdot$ uncertainty $L(\ln(p_T[\text{TeV}]), \ln(0.1), \ln(2.5)) \cdot L(\|y\|, 2, 3)\cdot$ uncertainty
16	$\sqrt{1 - L(\ln(p_T[\text{TeV}]), \ln(0.1), \ln(2.5))^2} \cdot \sqrt{1 - L(\|y\|, 0, 1.5)^2}\cdot$ uncertainty $\sqrt{1 - L(\ln(p_T[\text{TeV}]), \ln(0.1), \ln(2.5))^2} \cdot L(\|y\|, 1.5, 3)\cdot$ uncertainty
17	$\sqrt{1 - L(\ln(p_T[\text{TeV}]), \ln(0.1), \ln(2.5))^2} \cdot \sqrt{1 - L(\|y\|, 0, 1)^2}\cdot$ uncertainty $\sqrt{1 - L(\ln(p_T[\text{TeV}]), \ln(0.1), \ln(2.5))^2} \cdot L(\|y\|, 1, 3)\cdot$ uncertainty
18	$\sqrt{1 - L(\ln(p_T[\text{TeV}]), \ln(0.1), \ln(2.5))^2} \cdot \sqrt{1 - L(\|y\|, 0, 2)^2}\cdot$ uncertainty $\sqrt{1 - L(\ln(p_T[\text{TeV}]), \ln(0.1), \ln(2.5))^2} \cdot L(\|y\|, 2, 3)\cdot$ uncertainty

Where:

$$L(x, \text{min}, \text{max}) = \frac{x - \text{min}}{\text{max} - \text{min}}$$

for x in the range [min,max]

$$L(x, \text{min}, \text{max}) = 0 \text{ for } x < \text{min}$$

$$L(x, \text{min}, \text{max}) = 1 \text{ for } x > \text{max}$$

An extra sub-component completes them, such that the sum in quadrature of sub-components equals the original uncertainty

Results: NLOJet++ vs Unfolded Data (8 TeV)

(arXiv:1706.03192)

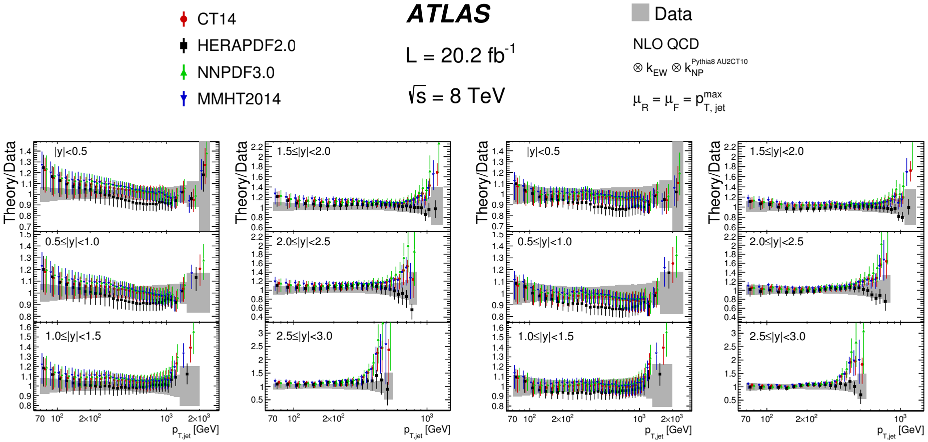

anti-k_t $R = 0.4$ anti-k_t $R = 0.6$

EW corrections at 13 TeV

- NLO pQCD predictions are corrected for the effects of γ and $W^{\pm}/Z$ interactions at the tree and 1-loop level
- The correction is defined as the ratio

$$\frac{\sigma\left(2\to 2,\mathrm{LO}^{(\mathrm{QCD})}+\mathrm{NLO}^{(\mathrm{EW})}\right)}{\sigma\left(2\to 2,\mathrm{LO}^{(\mathrm{QCD})}\right)}$$

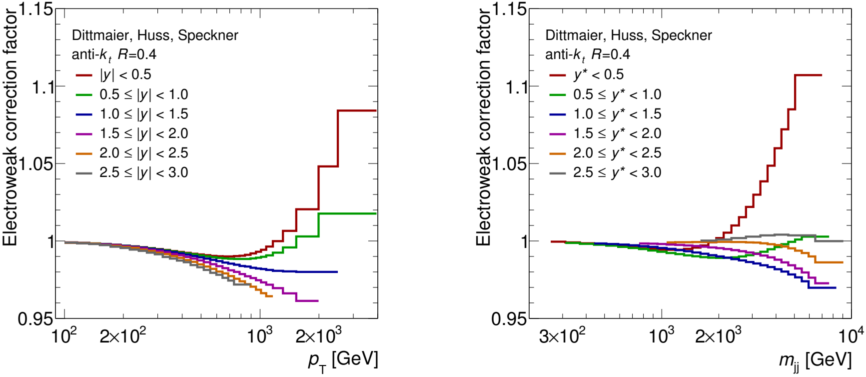

Unfolding Procedure

1. Matching impurity at reconstructed level ($\mathcal{P}_j$).
2. Migrations between neighbour $p_{\mathrm{T}}(m_{jj})$ bins ($\mathcal{A}_{ij}$).
3. Matching inefficiency at particle-level ($\mathcal{E}_i$).

$$N_i^{\text{unfolded}} = \sum_j N_j^{\text{reco}} \cdot \mathcal{P}_j \cdot \mathcal{A}_{ij} \,/\, \mathcal{E}_i$$